Gallium nitride based transistors

2001 J. Phys.: Condens. Matter 13 7139

(http://iopscience.iop.org/0953-8984/13/32/317)

INSTITUTE OF PHYSICS PUBLISHING JOURNAL OF PHYSICS: CONDENSED MATTER

J. Phys.: Condens. Matter **13** (2001) 7139–7157 PII: S0953-8984(01)25871-8

Gallium nitride based transistors

H Xing[1], S Keller[1], Y-F Wu[2], L McCarthy[1], I P Smorchkova[1], D Buttari[1], R Coffie[1], D S Green[1], G Parish[1], S Heikman[1], L Shen[1], N Zhang[1], J J Xu[3], B P Keller[2], S P DenBaars[1] and U K Mishra[1]

[1] Electrical and Computer Engineering Department, University of California, Santa Barbara, CA 93106, USA
[2] CREE Lighting Company, 340 Storke Road, Goleta, CA 93117, USA
[3] Gtran, 1153 Lawrence Drive, Newbury Park, CA 91320, USA

E-mail: hxing@ece.ucsb.edu

Received 15 June 2001
Published 26 July 2001
Online at stacks.iop.org/JPhysCM/13/7139

Abstract

An overview is presented of progress in GaN electronic devices along with recent results from work at UCSB. From 1995 to 2001, the power performance of AlGaN/GaN high electron mobility transistors (HEMT) improved from 1.1 to 11 W mm^{-1}, respectively. The disadvantage of the low thermal conductivity of the sapphire substrate was mitigated by flip-chip bonding onto AlN substrates, yielding large periphery devices with an output power of 7.6 W. A variety of HEMT amplifier circuits have been demonstrated. The first AlGaN/GaN heterojunction bipolar transistor (HBT) was demonstrated in 1998, with a current gain of about 3. By developing the technique of emitter regrowth, a current gain of 10 was achieved in both GaN BJTs and AlGaN/GaN HBTs. A common emitter current gain cutoff frequency of 2 GHz was measured. Critical issues involved in the growth of high quality AlGaN/(AlN)/GaN heterostructures and GaN:Mg by metal–organic chemical vapour deposition (MOCVD) and molecular beam epitaxy (MBE) and the device fabrication are discussed.

1. Introduction

The gallium nitride materials system has established itself as extremely important for next generation opto-electronics by filling the void in the opto-electronic spectrum from the green to the ultra-violet. This has created new markets in green LED traffic signals, full colour outdoor displays and promises the next great advance in lighting since the fluorescent lamp. The promise of electronic applications is primarily in the area of sources and amplifiers for communications and low loss switches in power conditioning applications. (Al, Ga, In)N based semiconductors promise both to add on to present silicon, GaAs and InP based

solid-state solutions for power amplifiers and to be a major component of a new power electronics technology. As members of the III–V nitride family, AlN, GaN, InN and their alloys are all wide bandgap materials, and can crystallize in both zinc blende and wurtzite polytypes. In cubic form, GaN and InN have direct bandgaps, while AlN is indirect. Wurtzite (Al, Ga, In)N forms a continuous and direct band gap alloy from 1.9 eV (InN) to 6.2 eV (AlN). GaN itself possesses a large band gap of 3.4 eV, a very high breakdown field (3×10^6 V cm^{-1}) and an extremely high peak (3×10^7 cm s^{-1}) and saturation velocity (1.5×10^7 cm s^{-1}) [1]. These properties in combination with the high band offset and the high electron mobility observed in AlGaN/GaN heterostructures (2019 cm^2 V^{-1} s^{-1}) [2], promise an excellent microwave power performance of GaN based heterojunction field effect transistors. Furthermore, the wurtzite crystal structure of group-III nitrides is highly piezoelectric, offering device design possibilities not accessible with common GaAs and InP based semiconductors. Due to the strong chemical bonds in the semiconductor crystal, GaN based devices are also promising for high temperature operation and applications under radiation exposure.

Historically, GaN was one of the first III–V-compound semiconductors to be studied. First reports on the epitaxy of GaN by halide vapour phase epitaxy date back to the year 1969 [3]. Due to the non-availability of a single crystalline GaN substrate, GaN films were typically deposited on sapphire substrates. Although years of intensive studies on GaN growth and its properties followed, the interest declined in the early 1980s, as several severe problems, preventing the utilization of GaN in electronic and opto-electronic devices, seemed to be impossible to overcome: the GaN films suffered from a very high n-type background carrier concentration and no p-type doping could be achieved. In the late 1980s high quality GaN films on sapphire substrates were reported in a two-step growth process, which resulted in a dramatic improvement of both the structural and the electrical properties of the GaN films [4]. In 1989, p-type GaN was obtained by post-growth LEEBI treatment of magnesium doped GaN films [5]. Three years later the LEEBI procedure was replaced by a post-growth thermal treatment [6]. The persistent work on group III nitrides, especially in Japan, resulted in an interest revival in nitride semiconductors all over the world.

A broad range of GaN electronic devices has been realized, including high electron mobility transistors (HEMTs), heterojunction bipolar transistors (HBTs), bipolar junction transistors (BJTs), Schottky and pin rectifiers and metal oxide semiconductor field effect transistors (MOSFETs). First, we present the progress in the AlGaN/(AlN)/GaN HEMT performance from a historic point of view and discuss critical issues involved in the process. Second, (Al)GaN bipolar transistor performance and related issues are addressed.

2. AlGaN/(AlN)/GaN HEMTs

The first AlGaN/GaN high electron mobility transistors (HEMTs) were demonstrated by Asif Khan *et al* in 1994 [7]. Devices with 0.25 μm gate length showed a current density (I_{dss}) of 60 mA mm^{-1} and a transconductance (g_m) of 27 mS mm^{-1}, but no microwave power performance had been reported. Today state-of-the-art AlGaN/GaN HEMTs and amplifiers exhibit an output power density as high as 11 W mm^{-1} [8] and a total output power of 51 W [9], respectively.

In order to obtain devices of high power ($P_{max} = V_{max} I_{max}/8$), the following parameters must be maximized for HEMTs, since current, $I = qn_s v$.

- Low leakage in buffer, demanding highly resistive epilayers with low defect density, i.e. intrinsic material with no compensation ideally.

- Breakdown voltage V_{br}, requiring high quality material, proper device design and proper surface passivation.
- Sheet charge density n_s, necessitating the maximization of the spontaneous and piezoelectric polarizations (P_{SE} and P_{PE}) thus maximizing the Al mole fraction without strain relaxation is required.
- Electron velocity v, demanding an reduced effective gate length (L_g) and gate length extension.
- Electron mobility μ, requiring the minimization of scattering centres due to dislocations, interface roughness and alloy disordering at the heterojunction.
- Thermal conductivity, necessary to remove the heat generated by devices. Possible solutions are thick GaN on sapphire or SiC substrates.

Based on the design rules above for AlGaN/(AlN)/GaN HEMTs-based power amplifiers several processes have to be developed: (1) growth of high quality semi-insulating GaN films, (2) growth of high quality AlGaN/(AlN)/GaN heterostructures and (3) nitride suitable device processing procedures. At UCSB, sapphire and insulating SiC have been chosen as the substrates, and both metal–organic chemical vapour deposition (MOCVD) and molecular beam epitaxy (MBE) (regrown on MOCVD templates) as the growth method. For MOCVD the precursors were trimethylgallium (TMGa), trimethylaluminium (TMAl) and ammonia (NH_3), and disilane (Si_2H_6) was used as the n-type dopant source. For MBE the active nitrogen was supplied by an EPI Unibulb nitrogen plasma source while conventional effusion cells were used for Ga and Al. Figure 1 presents the relationship between improved materials and device design and the device performance (using data primarily from UCSB).

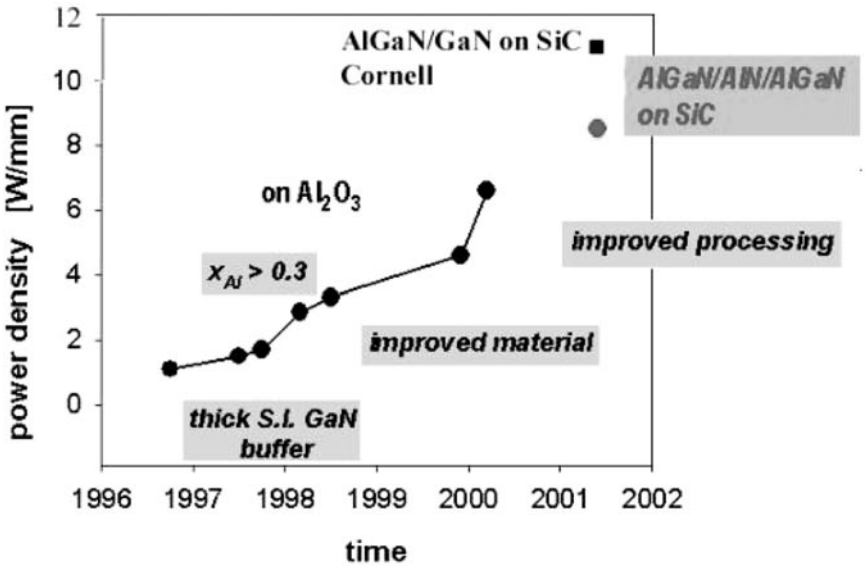

Figure 1. Progress in power density reported for AlGaN/GaN HEMTs from UCSB.

2.1. Semi-insulating GaN and early stage AlGaN/GaN HEMTs

In UCSB the GaN epitaxy was performed following the established two-step growth procedure by MOCVD, with sapphire as the substrate [10]. To fabricate semi-insulating films, the residual

background carrier concentration in the GaN films had to be reduced. In the past, the n-type conductivity of GaN layers had been mainly attributed to the formation of nitrogen vacancies in the crystal. More detailed investigations, though, suggested that oxygen impurities, rather than nitrogen vacancies, are the major source of residual electrons [11, 12]. Oxygen, if incorporated on the nitrogen site is a shallow donor in GaN. Water and oxygen are omnipresent impurities in the system. Both can either be present as impurities in the metal–organic precursors and gases or enter the system through leaks in the MOCVD system or during wafer loading. Another potential source is the sapphire substrate, since water forms during the sapphire (Al_2O_3) pre-treatment in hydrogen.

The influence of the wafer loading procedure and the sapphire pre-treatment on the residual background carrier concentration was investigated [13], and it was found that both contribute to the residual background carrier concentration in the films. By using *ex situ* baked sapphire substrates and inserting a long flush time after wafer loading, the residual carrier concentration in 3.2 μm GaN films could be reduced from $n_s = 1.3 \times 10^{13}$ cm^{-2} to $n_s = 7.2 \times 10^{12}$ cm^{-2}, which is equivalent to an average volume carrier concentration of $n = 2.2 \times 10^{16}$ cm^{-3}. The carrier concentration in the near surface region of the wafer was $n = 1 \times 10^{16}$ cm^{-3}, determined by C–V measurements using a mercury probe.

Besides system purity, the residual background carrier concentration depends on the growth conditions of the high temperature GaN layer. Generally, highly resistive films were obtained at reduced growth temperatures and/or reduced reactor pressures, characterized by a higher carbon impurity concentration in the films [14]. Under these conditions, the background donors were compensated by a deep acceptor, the so-called yellow level, appearing as a broad band in the photoluminescence (PL) spectrum at a wavelength of approximately 550 nm. Possibly, carbon impurities assist in the formation of gallium vacancies, which had been identified as source of the yellow luminescence [15].

For the fabrication of S.I. GaN base layers a two-step process was chosen: the first part of the layer was deposited at low pressure to compensate for the higher concentration of oxygen donors close to the sapphire/GaN interface by a higher concentration of deep acceptors; the second part of the layer was deposited at atmospheric pressure to ensure a low density of point defects in the GaN layer close to the AlGaN/GaN interface.

At the early stage of the AlGaN growth development, the AlGaN layers were typically deposited at a reduced reactor pressure of 76 Torr to suppress the pre-reactions between TMAl and NH_3, with a high NH_3 flow rate of 6 slm. Under such growth conditions step flow growth of AlGaN similar to GaN was observed for $x_{Al} < 0.25$. Films with higher Al mole fraction exhibited a grainlike structure (figure 2(c)).

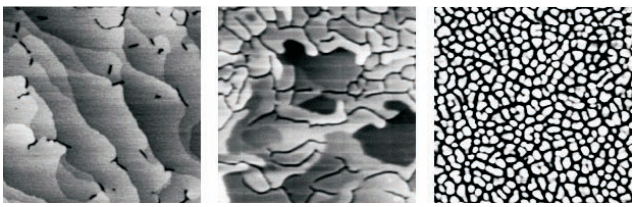

Figure 2. Atomic force microscopy images of 20 nm thick $Al_{0.35}Ga_{0.65}N$ layers grown on GaN by MOCVD with an ammonia flow of (a) 1.5 l min^{-1}, (b) 3 l min^{-1} and (c) 6 l min^{-1}. Island growth and defect formation in the AlGaN layer is suppressed at low NH_3 flows during growth.

The first AlGaN/GaN HEMTs at UCSB were fabricated from heterostructures consisting of 30 nm $Al_{0.15}GaN$ on a thin (0.3 μm) buffer on sapphire, intending to reduce the parallel conduction through the buffer. Devices were obtained by optical lithography and mesa isolation with Cl_2 reactive ion etching (RIE) [16]. Continuous wave (CW) power measurements were performed on wafer without cooling. At a frequency of 2 GHz, a class A output power density of 1.1 W mm^{-1} with a power added efficiency (PAE) of 18.6% was obtained, the first power data reported for a GaN based field effect transistor [17]. The output power was found to be limited by the serious heating of the device under operation and the poor electron transport in the channel. This is because a thin GaN base layer on sapphire has (i) high composite thermal impedance and (ii) poor crystalline quality. Increasing the thickness of GaN base layers, a CW power density of 1.57 W mm^{-1} at 4 GHz was demonstrated on HEMTs fabricated on a heterostructure consisting of 40 nm $Al_{0.15}Ga_{0.85}N$ on 2–3 μm semi-insulating GaN layers [18].

2.2. AlGaN/GaN HEMTs with higher Al composition

Following the design rules for high performance HEMTs, which dictate structures that yield a high sheet charge density with concomitant high mobility while maintaining a breakdown voltage appropriate for the application, further efforts were directed towards devices with higher Al content in the gating layer. The resulting higher band discontinuity should improve the carrier confinement, and the stronger spontaneous polarization and the piezoelectric effects contribute to a higher sheet charge density in the channel. In addition, the higher band gap of the AlGaN layer promised a higher composite breakdown field.

For an experimental investigation, AlGaN/GaN epitaxial films with identical layer structure of 2 μm S.I. GaN and 20 nm $Al_xGa_{1-x}N$ (3 nm UID spacer, 15 nm $Al_xGa_{1-x}N$:Si, 2 nm UID cap) were grown. First the Al mole fraction (x_{Al}) was varied. As expected, the sheet charge density increased with increasing Al content in the $Al_xGa_{1-x}N$ layer: for the chosen Al mole fractions of 15, 25, 35 and 50%, n_s values of 8×10^{12} cm^{-2}, 1×10^{13} cm^{-2}, 1.2×10^{13} cm^{-2} and 1.2×10^{13} cm^{-2} were measured. That the sheet carrier density remained constant at $x_{Al} > 35\%$ was attributed to a reduced Si-doping efficiency and the AlGaN grain growth at these high Al mole fractions. Due to the grain formation, the AlGaN layer relaxed, eliminating the piezoelectric contribution to the sheet carrier density. The electron mobility for the samples ranged between 1200 and 1000 cm^2 V^{-1} s^{-1} at 300 K.

The effect of the Al composition on the power performance was investigated with 25 and 50% Al content. The device performance is summarized in table 1. Although the $Al_{0.5}Ga_{0.5}N$/GAN HEMT suffered from the poor ohmic contact resistance, the output power density steadily increased with increasing Al mole fraction as predicted.

Table 1. HEMT performance versus Al content.

x_{Al}	L_g (μm)	Ohmic (Ω mm)	I_{dss} (A mm^{-1})	g_m (ms mm^{-1})	V_{br} (V)	P@4 GHz (W mm^{-1})	PAE (%)
0.25	0.9	0.5	1	255	∼230	1.9	24
0.5	0.7	1	1.05	220	>284	2.7	28

Short gate length devices were fabricated from $Al_{0.5}Ga_{0.5}N$/GaN heterostructures by electron beam lithography with T-gate technology (L_g was 0.25–0.28 μm, L_{gs} and L_{gd} were 0.6 and 0.75 μm, respectively). Due to the shorter channel, which results in a channel velocity closer to saturation, the saturation current was increased to 1.13 A mm^{-1}. The extrinsic

transconductance of 240 mS mm^{-1} was about the same as that for the devices fabricated by optical lithography and mostly limited by the relatively high ohmic contact resistance of 0.9–1 Ω mm. Small signal microwave characterization performed on devices with 100 μm gate width yielded current gain and power gain cutoff frequencies (f_t and f_{max}) of 52 and 82 GHz, respectively (limited by the ohmic contact resistance). When biased and tuned for maximum power at 18 GHz, the output power density reached a value of 3.3 W mm^{-1}, with a large signal gain, PAE and drain efficiency of 2.4 dB, 18.2% and 42.7%, respectively [19]. More recently, an output power of 5.1 W mm^{-1} at 26 GHz was demonstrated, with f_t, f_{max}, a linear gain and PAE of 60 GHz, 120 GHz, 10 dB and 25.6%, respectively [20].

The effect of the gate width on the power performance was investigated using $Al_{0.5}Ga_{0.5}N$/GaN HEMTs with 0.25 μm gate length. Increasing the gate width from 100 to 500 μm, a steady increase of the total output power from 0.35 to 1 W at 8 GHz was observed, whereas the power density decreased from 3.3 to 2 W mm^{-1}, respectively. This behaviour was attributed to the more severe self-heating for larger devices, emphasizing again the need for an efficient heat management [19].

2.3. HEMTs with improved AlGaN

Since the sheet carrier density saturation at higher Al mole fractions in the AlGaN layer and the accompanied current saturation in the devices observed in the previous set of experiments had been attributed to the grain growth of the $Al_xGa_{1-x}N$ layer at $x_{Al} > 0.25$ and the resulting strain relaxation, further growth experiments were undertaken in particular to optimize the growth conditions of AlGaN films with high Al content. The experiments revealed that grain formation in the $Al_xGa_{1-x}N$ layers could be prevented under conditions ensuring a high surface mobility of metal species, specifically at low ammonia flows during growth (figure 2). Under optimized conditions coherently strained $Al_xGa_{1-x}N$/GaN heterostructures were obtained up to $x_{Al} = 1$, with the $Al_xGa_{1-x}N$ layer growing in a step flow growth mode comparable to GaN (figure 2(a)). Since no relaxation in the $Al_xGa_{1-x}N$ layers occurred, the sheet carrier density now linearly increased with Al content in the $Al_xGa_{1-x}N$ layer and did not show any saturation as observed in the previous experiments (figure 3) [21]. The mobility of the 2 DEG, though, decreased with increasing Al content, in agreement with theoretical considerations. Following the model of Zhang and Singh [22], with increasing Al mole fraction the conduction band discontinuity, the strain and the piezoelectric field in the $Al_xGa_{1-x}N$ layer increase, resulting in a higher two-dimensional electron charge. However, the higher the sheet carrier density and the sheet charge, the closer the centroid of the 2DEG density is to the interface, and the more the electron transport is affected by the surface roughness and the alloy scattering. Further details on the effect of various growth parameters on the sheet carrier density and the mobility were discussed in [21].

For AlGaN/GaN HEMTs an intermediate Al composition of about 35% seemed most promising, typically resulting in a sheet carrier density of $\sim 1.2 \times 10^{13}$ cm^{-3} and a 2DEF mobility of $\sim$1250 cm^2 V^{-1} s^{-1} at 300 K for an $Al_{0.35}Ga_{0.65}N$ layer thickness of 18 nm (2.5 nm UID spacer, 10 nm $Al_{0.35}Ga_{0.65}N$:Si, [Si] $\sim 1 \times 10^{19}$ cm^{-3}, 5 nm UID cap) grown on 3 μm S.I. GaN. Devices with $\sim$0.7 μm gate length fabricated from these coherently strained $Al_{0.35}Ga_{0.65}N$/GaN heterostructures reached an output power density of 4.6 W mm^{-1} at 6 GHz, with a PAE of 40% when biased at 26 V. Devices with an output power density of 4.6 W mm^{-1} and a PAE of 44% (drain voltage 25 V) were obtained using a recessed gate process. When the same devices were tuned for optimum efficiency (drain voltage 23 V), the PAE reached values as high as 57% at an output power of 4.1 W mm^{-1} [23]. The measurements had been performed un-cooled on wafer using an active load-pull system.

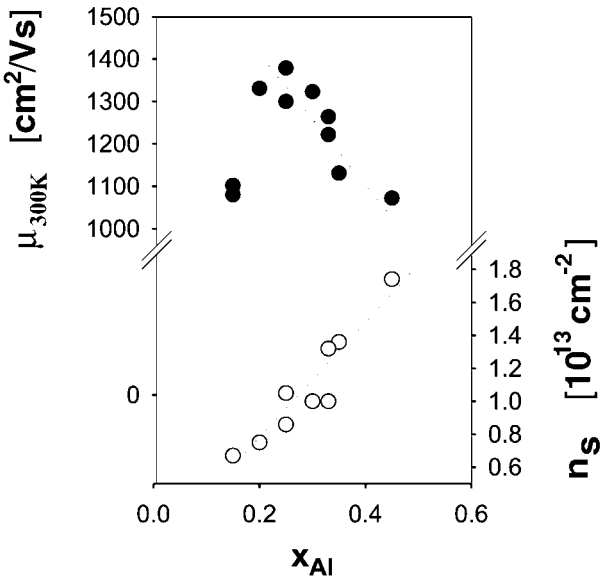

Figure 3. Dependence of the electron mobility (filled circles) and the sheet carrier density (open circles) measured at 300 K on the Al mole fraction in the $Al_xGa_{1-x}N$ layers.

However, although the power performance of the AlGaN/GaN on sapphire HEMTs at UCSB had been tremendously improved, the comparison to results obtained for AlGaN/GaN HEMTs on SiC in the same year pointed again towards the limitations resulting from the low thermal conductivity of the sapphire substrate. Thus, even higher power values of 6.8 W mm^{-1} at 10 GHz ($x_{Al} = 0.14$) [24, 25] and 9.1 W mm^{-1} at 8.2 GHz along with a PAE of 47% ($x_{Al} = 0.3$) [26] had been achieved by groups who fabricated AlGaN/GaN HEMTs on SiC substrates, combining the excellent device properties of GaN HEMTs with the advantages of a substrate with an almost ten times higher thermal conductivity ($\kappa_{SiC} = 4$ W cm^{-1} K^{-1}) in comparison to sapphire ($\kappa_{sapphire} = 0.41$ W cm^{-1} K^{-1}). Besides the importance of an efficient heat management, the results on SiC substrates re-emphasize the superior performance of devices with high Al content in the AlGaN layer.

2.4. Large periphery devices and amplifiers with thermal management through flip-chip bonding

Despite the superior performance of the devices fabricated on SiC substrates, a GaN HEMT on sapphire, with proper thermal management, appeared still as a strong candidate for practical applications considering the much lower cost and the larger available wafer size of the sapphire substrates, in particular for the fabrication of large periphery devices. To reduce the thermal limitations caused by the sapphire substrate, a flip-chip bonding approach of AlGaN/GaN-on-sapphire HEMTs onto AlN substrates was chosen at UCSB. Although somewhat lower than that of SiC, the thermal conductivity of AlN ($\kappa_{AlN} = 2.8$ W cm^{-1} K^{-1}) is still about seven times higher than that of sapphire. Due to the significantly improved heat dissipation, the channel current increased from 1.1 A mm^{-1} to 1.6 A mm^{-1} for 75 μm wide devices [27]. In collaboration with Nitres, Inc. (now CreeLighting), 1, 2, 4 and 6 mm devices were developed, using 10–40 gate fingers of 100–150 μm width. These devices exhibited output power levels

of 2.1, 3.2, 5.5 and 7.6 W, respectively, with PAEs of 35–53% at 4 GHz. Modifications in the device design to reduce the gate-feed resistance and to optimize the thermal management, resulted in an output power of 3.2 W for the 1 mm wide devices [28], which is close to the 3.9 W value reported for 1 mm GaN HEMTs on SiC [25], demonstrating the effectiveness of the thermal management scheme.

These developments in the GaN HEMT device technology enabled the fabrication of the first GaN-based broadband power amplifiers. Using the modified capacitive-division TWPA (travelling wave power amplifier) circuit topology, amplifiers with an output power of 3.6 W when biased at 18 V and 4.5 W when biased at 22 V were obtained at mid-band (4 GHz) [29]. Using a slightly different design, a transducer gain of up to 11.5 dB at 8 GHz, along with a bandwidth of 3–9 GHz, was achieved. The saturation power levels were about 32–35 dB m^{-1} for amplifiers using 1 and 2 mm wide devices, which are about twice as high as achievable with GaAs-based counterparts of the same size [30].

2.5. Performance improvement through 'defect' control

Although the AlGaN/GaN HEMT output power could be significantly improved through a careful heat management, the device performance analysis under AC and DC conditions suggested, that self-heating was not the only factor limiting the performance. Figure 4(a) shows the I–V characteristics of a AlGaN/GaN HEMT grown on sapphire under DC (14 millisecond) and pulsed (80 microsecond) gate drives, the latter one simulating AC operation conditions. The maximum current under pulsed gate drive is significantly smaller, and the knee voltage larger than those under DC gate drive. This phenomenon, called 'dispersion', was often observed and attributed to traps in the device structure. The dispersion reduced device output power and PAE due to the reduction in current and increase in knee voltage at high frequencies. A more severe dispersion was generally found for wafers with higher dislocation densities, higher point defect concentrations and/or plasma damaged surface [23], as AlGaN/GaN heterostructures are extremely sensitive to any surface treatment. Due to the spontaneous polarization and piezoelectric effects immanent for wurtzite GaN and AlGaN grown in the typical (0001) growth direction [31], a significant number of charged defects form on the surface of the AlGaN layer to ensure charge neutrality in the structure [32, 33]. In fact, AlGaN/GaN heterostructures with high 2DEG carrier densities ($>1 \times 10^{13}$ cm^{-3}) can be fabricated without any doping of the AlGaN layer due to the formation of a surface donor [34].

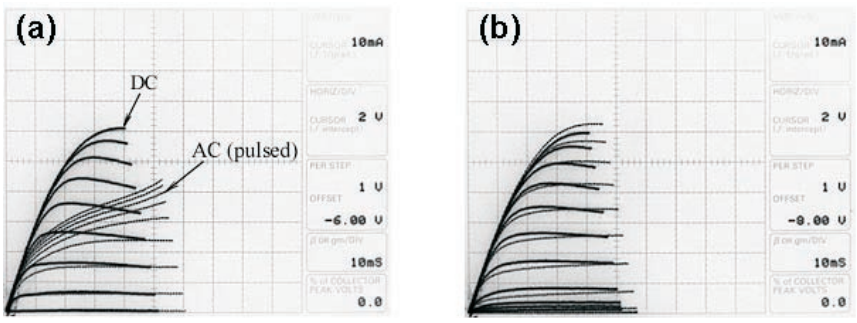

Figure 4. I–V characteristics of AlGaN/GaN HEMTs under DC and pulsed gate drives (simulating AC operation). (a) Significant dispersion due to traps and (b) negligible dispersion by passivating devices.

To address the dispersion problem, efforts were undertaken to further optimize the growth of the AlGaN/GaN heterostructures with respect to low point defect densities [14], and to develop processing schemes that pay special attention to the device surface.

Passivation of devices by dielectric material (such as Si_xN_y, Al_xN_y) has been very successful in dispersion suppression [35–40]. The I–V characteristic of AlGaN/GaN HEMTs passivated by Si_xN_y, is shown by figure 4(b) [41]. The DC and pulsed (AC) plots can be hardly distinguished. The saturation current density of the device was 1.2 A mm^{-1} and the maximum extrinsic transconductance 190 mS mm^{-1}. CW power measurements at 6 GHz were again performed un-cooled on wafer. Devices with 100 μm gate width were biased in class-AB mode with a quiescent drain current of 203 mA mm^{-1} and a source–drain voltage of 27 V. At the peak output power of 28.2 dB m^{-1}, the drain current was self-adjusted to 455 mA mm^{-1} with the input drive, resulting in a normalized power density of 6.6 W mm^{-1}. The corresponding large signal gain and PAE amounted to 9.2 dB and 47.2%. These are, by far, the best values reported for an AlGaN/GaN-on-sapphire HEMT measured on wafer, un-cooled to date. The results are largely limited by the low thermal conductivity of the sapphire substrate as discussed before and may be further improved by flip-chip bonding schemes and/or growth on SiC substrates, naturally possessing a very high thermal conductivity.

Combining all factors—depositing the GaN/AlGaN heterostructure on SiC substrates with high thermal conductivity, careful treatment of the AlGaN surface, plus additional heat management through wafer bonding onto AlN–AlGaN/GaN HEMTs exhibiting a power density of 9.8 W mm^{-1} with a PAE of 47% at 8 GHz were recently demonstrated by CreeLighting, Inc. [42]. Amplifier integrated circuits employing an 8 mm wide device delivered 51 W output power under operation, which is the highest power level for a GaN based HEMT or amplifier at C band to date [9].

2.6. Recessed gate AlGaN/GaN HEMTs

To improve HEMT performances, it is necessary to separate modulation of the charge under the gate from the effect of the gate on the region between the gate and the drain. Gate recess is the widely used technology in other III–V semiconductors. An ion-assisted etch process offers the possibility of better control of the depth and profile of the recess over wet chemical etching. Due to the lack of knowledge about RIE gate recess processes on III nitrides, there have been limited reports on improvements on AlGaN/GaN HEMTs performance [43–46].

HEMT performance as a function of different gate recess depth was investigated on an $Al_{0.33}Ga_{0.67}N$/GaN heterostructure by MOCVD on SiC with an AlN nucleation layer, a 2 μm GaN buffer and 30 nm $Al_{0.33}Ga_{0.67}N$ (D Buttari *et al*, to be published). The actual AlGaN thickness was determined to be between 24 and 27 nm by CV measurements. The device geometries were $L_g = 0.9$ μm, $L_{gs} = 0.6$ μm, $L_{gd} = 1.9$ μm and $W = 150$ μm. The gate recess etch was performed just before evaporating gate metal, utilizing a low power Cl_2 RIE. The etching conditions were 15 W input power and 10 sccm flow of Cl_2 at 10 mTorr. Three different etching times (50, 100 and 150 s) were performed and compared to un-etched devices. The etch depth was measured by atomic force microscopy (AFM) and determined to be about 3 nm for the 100 s etch and about 9 nm for the 150 s etch. The high non-linearity in etching depth with respect to etching time may be related to the formation of a thin oxide layer at the surface. This non-linearity can be avoided by the introduction of an etch stop layer. An increase in extrinsic transconductance and a positive threshold shift were observed with an increase of etching time. The two terminal gate–drain leakage increased from about 0.01 mA mm^{-1} to 0.1 mA mm^{-1}. The destructive three-terminal breakdown voltage was about 120 V for all devices, etched and un-etched. The power measurements were performed

in class A/B at a frequency of 8 GHz. Power measurements revealed no trend with the increase of etching time. The low increase in leakage, and no change in breakdown voltage support the fact that a low power RIE etch is a viable solution for low damage gate recess etch.

2.7. AlGaN/AlN/GaN HEMTs

From the theoretical calculations [47], the alloy disorder scattering was shown to be limiting mobilities for AlGaN/GaN 2DEG at low temperatures. AlN/GaN heterostructures were then investigated by MBE [48, 49]. It was found that at 20 K the electron mobility in the AlN/GaN structure with $N_s = 1.6 \times 10^{13}$ cm^{-2} reached 13 380 cm^2 V^{-1} s^{-1} while the $Al_{0.27}Ga_{0.73}N$/GaN structure with slightly lower 2DEG sheet density of 1.4×10^{13} cm^{-2} displays a significantly lower electron mobility of 4350 cm^2 V^{-1} s^{-1}. GaN/AlN/GaN and AlGaN/AlN/GaN structures were investigated as well by Hall measurements. The detailed results can be found in [49]. A higher conductivity is expected by inserting a thin AlN layer because the high piezoelectric field in the AlN generates a dipole, which increases the effective band offset in the conduction band resulting in a higher 2DEG density, and the removal of the alloy scattering improves the electron mobility.

HEMTs were fabricated on the new structures containing $Al_{0.3}$GaN(25 nm)/AlN(1 nm)/GaN grown on SiC by MOCVD with both doped and undoped AlGaN barrier layers (L Shen *et al*, to be published). The performances of the devices are summarized in table 2. Compared with the typical Hall values of $Al_{0.3}$GaN/GaN, 1200 cm^2 V^{-1} s^{-1} with 1.1×10^{13} cm^{-2}, the higher sheet charge densities and mobilities were achieved. The class AB output power was measured on the uncooled wafer at RT. The recent discoveries on AlN/GaN heterostructures open a new exciting field for AlGaN/GaN HEMT technology.

Table 2. Data of AlGaN/AlN/GaN HEMTs.

	n_s ($\times 10^{13}$ cm^{-2})	μ (cm^2 V^{-1} s^{-1})	I_{dss} (A mm^{-1})	g_m (mS mm^{-1})	P@8 GHz (W mm^{-1})	PAE (%)
Undoped AlGaN	1.22	1520	0.67	180	8.1	23
Doped AlGaN	1.65	1716	0.67	200	8.47	28

3. (Al)GaN HBTs

As demonstrated in other III–V material systems, HBTs offer several important advantages over FETs, HBTs generally have better threshold uniformity, better device linearity and lower phase noise than FETs. In addition, the HBT structure inherently offers higher ratio of output current to parasitic capacitance. Another important application for the GaN bipolar transistor is in high voltage switching applications where it may be desirable to switch high voltages at relatively high frequencies. Due to the difficultly in growth and processing related to p-GaN and the small minority carrier lifetime, the development of GaN bipolar junction transistors has been slow. The first AlGaN/GaN HBT was demonstrated at UCSB in 1998, with a current gain of about 3. By developing the technique of emitter regrowth, a current gain of 10 was achieved in both GaN BJTs and AlGaN/GaN HBTs. The small signal RF performance of AlGaN/GaN HBTs was also measured here, having a common emitter current gain cutoff frequency of 2 GHz with an input carrier density of over 2.7 kA cm^{-2}. Both npn and pnp HBTs have been fabricated with emitter contact diameters in the range of 20–200 mm and DC current gains of 3–20 have been reported from the common-emitter or common-base mode and Gummel plots [50–62].

3.1. Device considerations

In an npn bipolar transistor, device performances have the following basic demands on material quality and device designs based on the current GaN technology, besides reduction of defects in general:

(i) high current gain:
  (a) high emitter injection coefficient, utilizing (Al, Ga, In)N heterojunctions;
  (b) long minority lifetime, demanding high quality p-(Al, Ga, In)N and proper device designs and
  (c) short base transit time, requiring long diffusivity of minority carriers and thin and/or graded base;

(ii) high breakdown voltage, necessitating low background doping in collector (e.g. UID $< 1 \times 10^{16}$ cm^{-3} is needed for GaN collector to support up to 1 kV) and

(iii) RF performance:
  (a) high early voltage, requiring high doping in the base and
  (b) low base resistance and contact resistance, demanding high doping in the base and superior etch and contact technologies on p-GaN.

The most difficult hurdles facing GaN HBT developers are associated with p-type (Mg doped) GaN. The acceptor most commonly used in Mg. Because Mg is a deep acceptor (110–200 meV) [63], the doping concentration to achieve sufficient carrier concentration is extremely high (about 1×10^{20} cm^{-3} dopants result in about 1×10^{18} cm^{-3} holes). In addition, holes in GaN, with four times the effective mass of electrons, have especially low mobilities about 5–20 cm^2 V^{-1} s^{-1}. Consequently, the base of an npn transistor has a low conductivity. The low conductivity of the base increases the parasitic base capacitance, R_{bb}, as well as contributing to the current crowding effect in the base–emitter junction. Additionally, the high Mg levels in the base are detrimental to the minority lifetime and therefore the current gain. The p-GaN surface is sensitive to etch damage, and the Cl_2 RIE etch most commonly used to access the base layer causes damage, which makes ohmic contacts difficult to achieve. Furthermore, the Mg memory effect is common to many GaN MOCVD reactors, thus it is difficult to control the placement of the emitter–base junction [64].

We have implemented several strategies to overcome these difficulties. Low damage etching in conjunction with extrinsic base regrowth has been developed to decrease the parasitic offset voltage associated with a base contact voltage drop and high resistance. The regrown emitter HBT has been demonstrated as an alternative fabrication method in which the emitter structure is selectively regrown, avoiding etch damage and other etch related difficulties. MBE growth of GaN:Mg was developed to eliminate the Mg memory effect related to MOCVD [65]. Figure 5 shows the SIMS measurements of Mg levels in npn structures grown by MOCVD and MBE. The plot clearly shows a large Mg decay tail past the Mg turned-off point in the MOCVD sample. The Mg doping profile is much sharper in the MBE sample. Another advantage of MBE over MOCVD when growing Mg-doped GaN is that no post-growth anneal is required to electrically activate the Mg atoms. The absence of hydrogen in the plasma-assisted MBE process makes this unnecessary. We have also found the MBE growth to be more reproducible and more uniform across the sample. However, the more recent TEM studies show inverted domains in MBE grown GaN:Mg layers (J Speck *et al*, to be published), which might have deteriorated the device performances.

However, a high emitter–collector leakage is commonly seen in the GaN HBTs. The leakage path has been found to be due to dislocations present in current GaN materials, with a typical density of 5×10^8 cm^{-2}. Because this leakage is not apparent in base–collector and

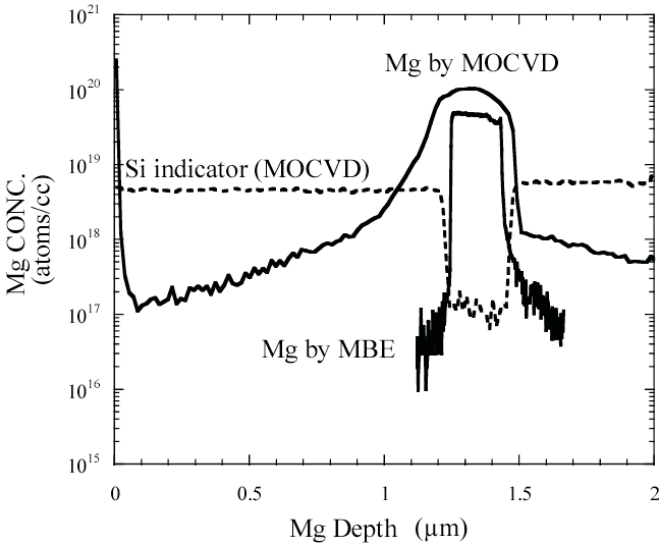

Figure 5. SIMS study of Mg profile in emitter of an npn structure grown by MOCVD and MBE.

base–emitter diode measurements, it can lead to misleading DC device characteristic curves in the common base and Gummel configurations.

3.2. The first AlGaN/GaN HBTs

AlGaN/GaN HBTs grown by MOCVD on sapphire substrates were demonstrated in 1998 for the first time [50]. Figure 6 shows a diagram of a completed device and the improvement resulting from a combination of a less-damaging etch and a regrown extrinsic base. A Si doped GaN sub-collector was followed by a 0.75 μm UID ($\sim 5 \times 10^{16}$ cm^{-3}) collector and a 2000 Å Mg doped base. The Si doped emitter ($n \sim 5 \times 10^{18}$ cm^{-3}) was grown with an $Al_{0.1}Ga_{0.9}N$ barrier layer to increase emitter injection efficiency into the strongly doped base. In order to reduce base resistance and overcome the difficulties of processing on non-uniform GaN layers, a thick base was chosen. The selectively regrown base was intended to reduce bulk resistivity under the contact and repair damage caused by a chlorine dry etch; it is believed that this damage creates nitrogen vacancies near the surface acting as donors and thus seriously degrades the p-contact quality.

The transistor was fabricated by masking the etched emitter mesa with a growth-selective dielectric. Al_xN_y was used for this purpose, as it was chemically inert in the reducing hydrogen ambient of MOCVD, as well as electrically inactive should it incorporate in the active device. Other masks including SiO_2 and Si_xN_y were found to be unstable, resulting in the doping of active layers by the mask. The common emitter I–V characteristics suggest a high early voltage due to acceptor doping in the base of approximately 4×10^{19} cm^{-3} resulting in a hole concentration of the order of 1×10^{18} cm^{-3}. The devices were operated at room temperature (RT) out to 40 V, exhibiting a beta of 3 and an offset voltage of over 5 V.

Although the regrown base buried the damaged base surface, the damaged material still formed a barrier to current flow into the active device. The subsequent development of etch recipes that reduced the extent of the damage used in conjunction with a regrown base has significantly improved base contacts (figure 6(b)).

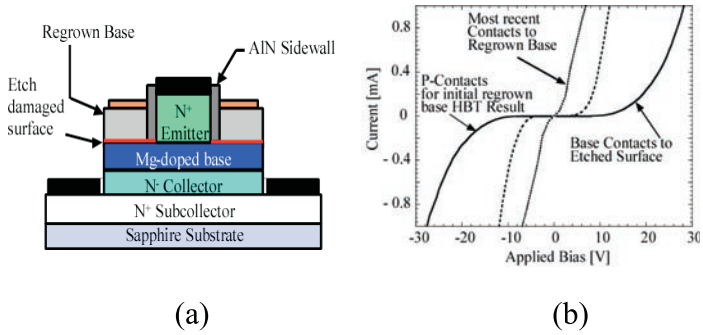

Figure 6. (a) A complete device with regrown base and (b) comparison of base contacts to the etched surface and to the regrown base.

The offset voltage is the collector bias in the common emitter mode where the net collector current becomes positive. At this point, both the base–emitter and base–collector diodes are forward biased. Large offsets in GaN bipolar transistors are caused by a strong asymmetry due to base contact voltage barriers ranging from 1 to 10 V. The non-linearity in the current–voltage relationship of the base contact results in a disparity between the voltage of the base under the base contact and under the emitter. The full explanation can be found in [66].

3.3. Regrown emitter HBTs

In order to reduce the etch damage to the p-GaN base and eliminate the influence on the emitter–base junction placement from the memory effect of Mg in MOCVD, the technique of a selectively regrown emitter has been developed. The regrown emitter device also uses the Al_xN_y dielectric regrowth mask to protect the base contact area and avoid compensating the active base. The emitter structure is then grown selectively by MOCVD. The growth mask is removed, and device processing completed with the conventional Cl_2 RIE to access the collector. Emitter and collector contacts are Ti/Al/Ni/Au, while the base contacts are Pd/Au. SIMS study shows that the regrown emitter technique indeed results in a sharp Mg profile at the emitter–base junction (figure 7(a)) [67], allowing an accurate base emitter junction placement for HBTs.

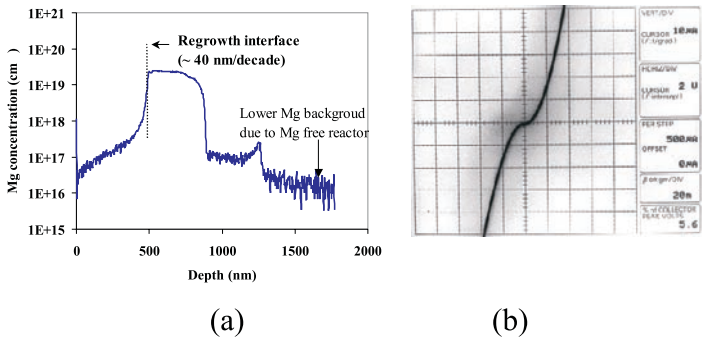

Figure 7. (a) Mg profile in an npn structure and (b) base contacts, resulting from the regrown emitter technique.

The first AlGaN/GaN HBTs using the regrowth emitters were demonstrated in 1999 [51]. The device had a Si doped GaN sub-collector followed by a 0.75 μm UID ($\sim 5 \times 10^{16}$ cm^{-3}) collector and a 2000 Å Mg doped base ($N_A \sim 5 \times 10^{18}$ cm^{-3}) all grown by MOCVD. After a Si_xN_y dielectric mask was patterned on the base–collector, $\sim$2000 Å $Al_{0.1}GaN$ doped with Si ($\sim 5 \times 10^{18}$ cm^{-3}) was selectively regrown by MOCVD. The RT common emitter operation up to 30 V showed a beta of 1.5 and an offset voltage of $\sim$5 V. The low current gain was found because of the thick base and the defected emitter–base junction resulting from the regrowth technique.

The base thickness was then reduced to 1000 Å to reduce the minority carrier transit time across the base and also ensure a reasonable GaN:Mg base resistance. With an improved process on the regrowth technique, both GaN:Si ($\sim 5 \times 10^{18}$ cm^{-3}) and $Al_{0.06}GaN$:Si ($\sim 1.5 \times 10^{18}$ cm^{-3}) emitters were selectively regrown on a base–collector structure ($\sim$1000 Å GaN doped with Mg $\sim 2 \times 10^{19}$ cm^{-3} and $\sim$7000 Å UID GaN with $N_D \sim 2 \times 10^{16}$ cm^{-3}) all by MOCVD (H Xing *et al*, to be published). Figure 7(b) shows that base contact characteristics were improved over the etched emitter device (figure 6(b)). Common emitter characteristics at room temperature of BJTs and HBTs show comparable current gains of 6–10 (figures 8(a) and 8(b)), and low offset voltage due to the high quality ohmic contacts by avoiding etching to reveal the p-type base. Both kinds of device were operated up to $\sim$100 V, showing low output conductance and an early voltage >400 V. Figures 9(a) and 9(b) shows the I–V characteristics of emitter–base diodes. The BJTs exhibited a low breakdown of the regrown emitter–base junction, while the HBTs shows much more ideal pn diode characteristics. However why the $Al_{0.06}GaN$:Si emitters greatly suppressed the leakage current of emitter–base diodes is still under investigation. Since the BJTs and HBTs were processed on the same wafer, the comparable current gains between them are attributed to the unknown recombination loss in the regrown emitter–base junction, which is directly related to the surface treatment before the emitter regrowth and the growth dynamics.

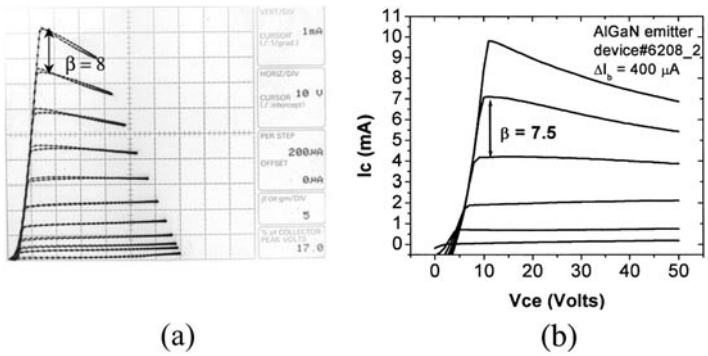

Figure 8. Common-emitter I–V characteristics of (a) a GaN BJT and (b) an $Al_{0.06}GaN$/GaN HBT.

To overcome the difficulties with revealing p-type GaN using RIE, photo-electro-chemical (PEC) wet etch techniques show promise [68, 69]. This etch allows selectivity of etching the n-type emitter over the p-type base. However, the etch stop becomes less effective when the etch stop layer thickness, W_b is less than L_n, the diffusion length of electrons in the base, which is unfortunately the case for bipolar transistor structures.

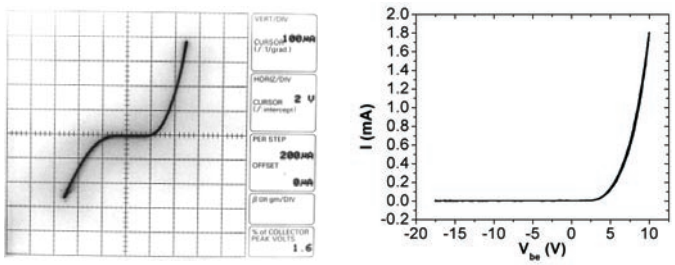

Figure 9. Emitter-base diodes of (a) a GaN BJT and (b) a $Al_{0.06}GaN/GaN$ HBT.

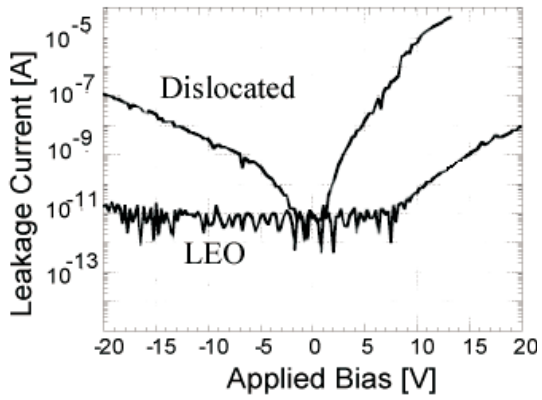

Figure 10. Emitter–collector leakage current of LEO window compared to wing region.

3.4. HBTs and LEO and emitter–collector leakage

Both the regrown emitter and etched emitter structures suffer from emitter–collector leakage associated with threading dislocations (TDs). Due to the lattice mismatch between GaN and sapphire or SiC, thin GaN films ($\sim$2 μm) grown on these substrates have a TD density of the order of 5×10^8 cm^{-2}. To investigate the connection between TDs, doping and collector–emitter leakage currents, devices were fabricated on HBT structures regrown by MBE on an LEO substrate [54]. The emitter is $Al_{0.1}Ga_{0.9}N$:Si doped 1×10^{18} cm^{-3} with a GaN:Si emitter contact layer, and the base layer is 100 nm GaN:Mg doped 5×10^{19} cm^{-3}. The collector–emitter leakage of adjacent devices was tested (figure 10) and was seen to drop by four orders of magnitude on the dislocation wing relative to the dislocated window. Although the leakage is reduced, the gain of devices in the wing region is comparable to devices in the window regions. This result suggests that although dislocations are the dominating cause of collector–emitter leakage in these devices, at the present levels (10^8 cm^{-2}) they are not related to the dominant recombination mechanism in the base. Further, the substrate is several times thicker (tens of microns, causing reduction of TD density) as opposed to the typical two microns for a standard template growth on sapphire. The cause of this leakage was then found to be the localized compensation of the neutral base around threading dislocations (TDs) [70]. The result of this leakage in extreme cases is a device that is shorted from collector to emitter.

This isolated leakage path can result in the misleading situation in which both the base–emitter and base–collector diodes appear to be rectifying when tested individually, while in fact the active device is shorted. Low base conductance adds to the problem by creating a disparity between the bias condition at the pads and in the intrinsic device where the leakage occurs. Under such circumstance, the transistor current cannot be distinguished from the leakage current. For these reasons, some of the usual methods of device characterization tend to yield erroneous results. Gummel plots, for instance, often show collector current with very little or not base current. A corresponding common emitter characteristic of the device shows that indeed much of the current is leakage

3.5. AlGaN/GaN HBTs small signal RF performance and pnp HBTs

Though there are many difficulties associated with p-GaN as base layers in bipolar structures, the small signal RF characteristics of an AlGaN/GaN HBT were demonstrated [71]. Devices were grown by MBE on GaN templates grown by MOCVD, consisting of a 500 nm GaN:Si (10^{18} cm^{-3}) subcollector followed by a 500 nm UID GaN collector. The base was 100 nm GaN:Mg (5×10^{19} cm^{-3}) followed by an abrupt heterojunction $Al_{0.1}Ga_{0.9}N$ (40 nm Si doped 10^{18} cm^{-3}) emitter capped with 10 nm of GaN:Si as a contact layer. The devices had a common emitter current gain cutoff frequency of 2 GHz with an input current density of over 2.7 kA cm^{-2}. The roll-off of the short-circuit current gain of the device was more gradual than 20 dB decade^{-1}, which was proposed because of the distributed nature of the base–collector parasitic capacitance caused by a high sheet resistance in the base and high base contact resistances.

The study on the depletion region in the presence of deep dopants, Mg in GaN, showed it is similar to the well studied case of a material doped both with shallow dopants and deep traps. Dispersion effects will result from the time required for the dopant to change ionization states [72]. Therefore, the npn bipolar transistors will suffer from these dispersion effects, resulting in a low early voltage at RF frequency. Pnp GaN HBTs benefit from the shallow dopant nature of Si in GaN, which facilitates the device processing and achieves a lower base resistance and a high RF early voltage. Some preliminary results on pnp GaN HBTs have been reported [62, 73, 74].

4. Conclusions

Over the past 7 years, the power performance of AlGaN/GaN HEMTs has improved tremendously. Difficulties in the MOCVD growth of the AlGaN/(AlN)/GaN heterostructures were overcome and the understanding of the physics of the semiconductor heterostructures reached a more mature level. More lately AlGaN/GaN HBTs have been demonstrated. In addition, device fabrication processes such as contact schemes and etching procedures were improved. Although GaN based power devices outperform present silicon, GaAs or InP based components already today, the devices have still not reached the calculated performance limit of 25 W mm^{-1} power density. Further concerted efforts in the device design and fabrication as well as in the understanding of the device physics will be needed to achieve this goal.

Acknowledgments

The work on AlGaN/GaN electronics at UCSB was supported by ONR through contacts supervised by Dr C Wood and Dr J Zolper and by AFOSR through contracts monitored by Dr G Witt.

References

[1] Gelmont B, Kim K and Shur M 1993 Monte Carlo simulation of electron transport in gallium nitride *J. Appl. Phys.* **74** 1818–21

[2] Gaska R, Yang J W, Osinsky A, Chen Q, Asif Khan M, Orlov A O, Snider G L and Shur M S 1998 Electron transport in AlGaN–GaN heterostructures grown on 6H-SiC substrates *Appl. Phys. Lett.* **72** 707–9

[3] Tietjen H P M A J J 1969 The preparation and properties of vapor-deposited single-crystal-line GaN *Appl. Phys. Lett.* **15** 327

[4] Amano H, Sawaki N, Akasaki I and Toyoda Y 1986 Metalorganic vapor phase epitaxial growth of a high quality GaN film using an AlN buffer layer *Appl. Phys. Lett.* **48** 353–5

[5] Amano H, Kito M, Hiramatsu K and Akasaki I 1989 p-type conduction in Mg-doped GaN treated with low-energy electron beam irradiation (LEEBI) *Japan J. Appl. Phys. Lett.* **28** L2112–14

[6] Nakamura S, Iwasa N, Senoh M and Mukai T 1992 Hole compensation mechanism of p-type GaN films *Japan. J. Appl. Phys.* **31** 1258–66

[7] Asif Khan M, Kuznia J N, Olson D T, Schaff W J, Burm J W and Shur M S 1994 Microwave performance of a 0.25 mu m gate AlGaN/GaN heterostructure field effect transistor *Appl. Phys. Lett.* **65** 1121–3

[8] Eastman J A *2nd GaN Electronics Workshop (Santa Barbara, CA, 2001)*

[9] Wu Y F, Chavarkar P M, Moore M, Parikh P, Keller B P and Mishra U K 2000 A 50-W AlGaN/GaN amplifier *Int. Electron Devices Meeting (San Francisco, CA, 2000)*

[10] Keller B P *et al* 1995 Metalorganic chemical vapor deposition growth of high optical quality and high mobility GaN *Proc. 7th Biennial Workshop on Organometallic Vapor Phase Epitaxy (Fort Meyers, FL, 1995)*

[11] Seifert W, Franzheld R, Butter E, Sobotta H and Riede V 1983 On the origin of free carriers in high-conducting n-GaN *Cryst. Res. Technol.* **18** 383–90

[12] Chung B C and Gershenzon M 1992 The influence of oxygen on the electrical and optical properties of GaN crystals grown by metalorganic vapor phase epitaxy *J. Appl. Phys.* **72** 651–9

[13] Keller S, Yi-Feng W, Parish G, Naiqian Z, Xu J J, Keller B P, DenBaars S P and Mishra U K 2001 Gallium nitride based high power heterojunction field effect transistors: process development and present status at UCSB *IEEE Trans. Electron Devices* **48** 552–9

[14] Parish G, Keller S, Denbaars S P and Mishra U K 2000 SIMS investigations into the effect of growth conditions on residual impurity and silicon incorporation in GaN and $Al_xGa_{1-x}N$ *Proc. 9th Biennial Workshop on Organometallic Vapor Phase Epitaxy (Ponte Vedra Beach, FL, 2000)*

[15] Saarinen K *et al* 1997 Observation of native Ga vacancies in GaN by positron annihilation *Phys. Rev. Lett.* **79** 3030–3

[16] Wu Y F, Keller B P, Keller S, Kapolnek D, Kozodoy P, Denbaars S P and Mishra U K 1996 Very high breakdown voltage and large transconductance realized on GaN heterojunction field effect transistors *Appl. Phys. Lett.* **69** 1438–40

[17] Wu Y F, Keller B P, Keller S, Kapolnek D, Denbaars S P and Mishra U K 1996 Measured microwave power performance of AlGaN/GaN MODFET *IEEE Electron Device Lett.* **17** 455–7

[18] Wu Y F, Keller S, Kozodoy P, Keller B P, Parikh P, Kapolnek D, Denbaars S P and Mishra U K 1997 Bias dependent microwave performance of AlGaN/GaN MODFET's up to 100 V *IEEE Electron Device Lett.* **18** 290–2

[19] Mishra U K, Wu Y F, Keller B P, Keller S and Denbaars S P 1998 GaN microwave electronics *1997 Topical Symp. on Millimeter Waves (Kanagawa, Japan)*

[20] Wu Y-F, Chavarkar P, Moore M, Parikh P and Mishra U K 2001 *2nd GaN Electronics Workshop (Santa Barbara, CA, 2001)*

[21] Keller S, Parish G, Fini P T, Hiekman S, Chen C H, Zhang N, DenBaars S P, Mishra U K and Wu Y F 1999 Metalorganic chemical vapor deposition of high mobility AlGaN/GaN heterostructures *J. Appl. Phys.* **86** 5850–7

[22] Zhang Y and Singh J 1999 Charge control and mobility studies for an AlGaN/GaN high electron mobility transistor *J. Appl. Phys.* **85** 587–94

[23] Wu Y F, Keller B P, Keller S, Xu J J, Thibeault B J, Denbaars S P and Mishra U K 1999 GaN-based FETs for microwave power amplification *IEICE Trans. Electron.* **E82-C** 1895–905

[24] Sheppard S T 1998 High power GaN/AlGaN HEMTs on silicon carbide *56th Annu. Device Research Conf. (1998)*

[25] Sheppard S T, Doverspike K, Pribble W L, Allen S T, Palmour J W, Kehias L T and Jenkins T J 1999 High-power microwave GaN/AlGaN HEMTs on semi-insulating silicon carbide substrates *IEEE Electron Device Lett.* **20** 161–3

[26] Wu Y F, Kapolnek D, Ibbetson J, Zhang N Q, Parikh P, Keller B P and Mishra U K 1999 High Al-content

AlGaN/GaN HEMTS on SiC substrates with very high power performance *Int. Electron. Devices Meeting (Washington, DC, 1999)*

[27] Thibeault B J, Keller B P, Fini P, Mishra U K, Nguyen C, Nguyen N X and Le M 1997 High performance and large area flip-chip bonded AlGaN/GaN MODFETs *Int. Electron. Devices Meeting (Washington, DC, 1997)*

[28] Wu Y F, Thibeault B J, Xu J J, York R A, Keller S, Keller B P and Mishra U K 1999 GaN HEMTs grown of sapphire substrates for microwave power amplification *Proc. 57th Annual Device Research Conf. (Santa Barbara, CA, 1999)*

[29] Xu J J, Yi-Feng W, Keller S, Heikman S, Thibeault B J, Mishra U K and York R A 1999 1–8-GHz GaN-based power amplifier using flip-chip bonding *IEEE Microw. Guid. Wave Lett.* **9** 277–9

[30] Wu Y F, York R A, Keller S, Keller B P and Mishra U K 1999 3–9-GHz GaN-based microwave power amplifiers with *L–C–R* broad-band matching *IEEE Microw. Guid. Wave Lett.* **9** 314–16

[31] F Bernardini V F and Vanderbilt D 1999 Spontaneous polarization and piezoelectric constants of III–V nitrides *Phys. Rev.* B **56** R10 024–7

[32] Ibbetson J P, Fini P T, DenBaars S P and Mishra U K 1999 *41st Electronic Materials Conf. (Santa Barbara, 1999)*

[33] Ambacher O *et al* 1999 Two-dimensional electron gases induced by spontaneous and piezoelectric polarization charges in N- and Ga-face AlGaN/GaN heterostructures *J. Appl. Phys.* **85** 3222–33

[34] Smorchkova I P, Elsass C R, Ibbetson J P, Vetury R, Heying B, Fini P, Haus E, DenBaars S P, Speck J S and Mishra U K 1999 Polarization-induced charge and electron mobility in AlGaN/GaN heterostructures grown by plasma-assisted molecular-beam epitaxy *J. Appl. Phys.* **86** 4520–6

[35] Vetury R, Zhang N Q, Keller S and Mishra U K 2001 The impact of surface states on the DC and RF characteristics of AlGaN/GaN HFETs *IEEE Trans. Electron Devices* **48** 560–6

[36] Eastman L F *et al* 2001 Undoped AlGaN/GaN HEMTs for microwave power amplification *IEEE Trans. Electron Devices* **48** 479–85

[37] Boudart B, Gaquiere C, Guhel Y, de Jaeger J C and Poisson M A 2001 Electrical effects of SiN_x deposition on GaN MESFETs *Electron. Lett.* **37** 527–8

[38] Green B M, Chu K K, Chumbes E M, Smart J A, Shealy J R and Eastman L F 2000 The effect of surface passivation on the microwave characteristics of undoped AlGaN/GaN HEMTs *IEEE Electron Device Lett.* **21** 268–70

[39] Jong-Soo L, Vescan A, Wieszt A, Dietrich R, Leier H and Young-Se K 2001 Small signal and power measurements of AlGaN/GaN HEMT with SiN passivation *Electron. Lett.* **37** 130–2

[40] Prunty T R, Smart J A, Chumbes E N, Ridley B K, Eastman L F and Shealy J R 2000 Passivation of AlGaN/GaN heterostructures with silicon nitride for insulated gate transistors *IEEE/Cornell Conf. on High Performance Devices (Ithaca, NY, 2000)*

[41] Zhang N Q *et al* 6.6-Watt/mm AlGaN HEMTs on sapphire substrate, to be published

[42] Yi-Feng W, Kapolnek D, Ibbetson J P, Parikh P, Keller B P and Mishra U K 2001 Very-high power density AlGaN/GaN HEMTs *IEEE Trans. Electron Devices* **48** 586–90

[43] Burm J, Schaff W J, Martin G H, Eastman L F, Amano H and Akasaki I 1997 Recessed gate GaN MODFETs *Topical Workshop on III–V Nitrides (Nagoya, Japan, 1997)*

[44] Breitschadel O, Kuhn B, Scholz F and Schweizer H 1999 Minimization of leakage current of recessed gate AlGaN/GaN HEMTs by optimizing the dry-etching process *J. Electron. Mater.* **28** 1420–3

[45] Egawa T, Ishikawa H, Jimbo T and Umeno M 1999 Recessed gate AlGaN/GaN MODFET on sapphire grown by MOCVD *Proc. Int. Electron Devices Meeting (Washington, DC, 1999)*

[46] Ching-Hui C, Keller S, Haberer E D, Zhang L, Danssaars S P, Hu E L and Mishra U K 1999 Cl_2 reactive ion etching for gate recessing of AlGaN/GaN field-effect transistors *Proc. 43rd Int. Conf. on Electron, Ion and Photon Beam Technology and Nanofabrication (Marco Island, FL, 1999)*

[47] Jena D, Smorchkova I P, Elsass C, Gossard A C and Mishra U K 2001 Electron transport and intrinsic mobility limits in two-dimensional electron gases of III–V nitride heterostructures, to be published

[48] Smorchkova I P, Keller S, Heikman S, Elsass C R, Heying B, Fini P, Speck J S and Mishra U K 2000 Two-dimensional electron-gas AlN/GaN heterostructures with extremely thin AlN barriers *Appl. Phys. Lett.* **77** 3998–4000

[49] Smorchkova I P *et al* 2001 AlN/GaN and (Al,Ga)N/AlN/GaN two-dimensional electron gas structures grown by plasma-assisted molecular beam epitaxy, to be published

[50] McCarthy L S, Kozodoy P, Rodwell M, DenBaars S and Mishra U K 1999 First demonstration of an AlGaN/GaN heterojunction bipolar transistor *Proc. Int. Symp. on Compound Semiconductors (Nara, Japan)*

[51] Limb J B, McCarthy L, Kozodoy P, Xing H, Ibbetson J, Smorchkova Y, DenBaars S P and Mishra U K 1999 AlGaN/GaN HBTs using regrown emitter *Electron. Lett.* **35** 1671–3

[52] Limb J B, Xing H, Moran B, McCarthy L, DenBaars S P and Mishra U K 2000 High voltage operation (>80 V) of GaN bipolar junction transistors with low leakage *Appl. Phys. Lett.* **76** 2457–9
[53] Xing H, McCarthy L, Keller S, DenBaars S P and Mishra U K 2000 *27th Int. Symp. on Compound Semiconductors (Monterey, CA, 2000)*
[54] McCarthy L, Smorchkova Y, Fini P, Xing H, Rodwell M, Speck J, DenBaars S and Mishra U 2000 HBT on LEO GaN *Proc. 58th DRC: Device Research Conf. (Denver, CO, 2000)*
[55] Yoshida S and Suzuki J 1999 High-temperature reliability of GaN metal semiconductor field-effect transistor and bipolar junction transistor *J. Appl. Phys.* **85** 7931–4
[56] Cao X A *et al* 2000 High current, common-base GaN/AlGaN heterojunction bipolar transistors *Electrochem. Solid-State Lett.* **3** 144–6
[57] Dang G *et al* 2000 Npn AlGaN/GaN heterojunction bipolar transistors and GaN bipolar junction transistors with regrown c-doped GaAs in the base regions *Solid-State Electron.* **44** 2097–100
[58] Huang J J, Caruth D, Feng M, Lambert D J H, Shelton B S, Wong M M, Chowdhury U, Zhu T G, Keon H K and Dupuis R D 2001 Room and low temperature study of common emitter current gain in AlGaN/GaN heterojunction bipolar transistors *Electron. Lett.* **37** 393–5
[59] Lambert D J H *et al* 2000 The growth of AlGaN/GaN heterojunction bipolar transistors by metalorganic chemical vapor deposition *Proc. 10th Int. Conf. on Metalorganic Vapor Phase Epitaxy (Sapporo, Japan, 2000)*
[60] Ren F *et al* 2000 GaN/AlGaN fabrication *Workshop on Wide Bandgap Bipolar Devices (Panama City Beach, FL, 2000)*
[61] Shelton B S *et al* 2001 Selective area growth and characterization of AlGHaN/GaN heterojunction bipolar transistors by metalorganic chemical vapor deposition *IEEE Trans. Electron Devices* **48** 490–4
[62] Zhang A P *et al* 2000 Direct-current characteristics of pnp AlGaN/GaN heterojunction bipolar transistors *Appl. Phys. Lett.* **76** 2943–5
[63] Kozodoy P, Huili X, DenBaars S P, Mishra U K, Saxler A, Perrin R, Elhamri S and Mitchel W C 2000 Heavy doping effects in Mg-doped GaN *J. Appl. Phys.* **87** 1832–5
[64] Ohba Y and Hatano A 1994 A study on strong memory effects for Mg doping in GaN metalorganic chemical vapor deposition *Proc. 7th Int. Conf. on Metalorganic Vapor Phase Epitaxy (Yokohama, Japan, 1994)*
[65] Smorchkova I P, Haus E, Heying B, Kozodoy P, Fini P, Ibbetson J P, Keller S, DenBaars S P, Speck J S and Mishra U K 2000 Mg doping of GaN layers grown by plasma-assisted molecular-beam epitaxy *Appl. Phys. Lett.* **76** 718–20
[66] McCarthy L S *et al* 2001 GaN HBT: toward an RF device *IEEE Trans. Electron Devices* **48** 543–51
[67] Xing H, Smorchkova I P, Kozodoy P, Keller S, DenBaars S P and Mishra U K 2001 Memory effect and redistribution of Mg into sequentially regrown GaN layer by metal organic chemical vapor deposition, to be published
[68] Stonas A R, Kozodoy P, Marchand H, Fini P, DenBaars S P, Mishra U K and Hu E L 2000 Backside-illuminated photoelectrochemical etching for the fabrication of deeply undercut GaN structures *Appl. Phys. Lett.* **77** 2610–12
[69] Adesida I, Youtsey C, Ping A T, Khan F, Romano L T and Bulman G 1999 Dry and wet etching for group III nitrides *MRS Internet J. Nitride Semicond. Res.* **4S1**
[70] McCarthy L, Smorchkova I, Xing H, Fini P, Keller S, Speck J, DenBaars S P, Rodwell M J W and Mishra U K 2001 Effect of threading dislocations on AlGaN/GaN heterojunction bipolar transistors *Appl. Phys. Lett.* **78** 2235–7
[71] McCarthy L, Smorchkova I P, Fini P, Rodwell M J W, Speck J, DenBaars S P and Mishra U K 2001 Small signal RF performance of AlGaN/GaN heterojunction bipolar transistors, to be published
[72] Kozodoy P, DenBaars S P and Mishra U K 2000 Depletion region effects in Mg-doped GaN *J. Appl. Phys.* **87** 770–5
[73] Peartson S J and Ren F 2000 GaN electronics *Adv. Mater.* **12** 1571–80
[74] Parikh P 2000 *IEEE/Cornell Conf. on High Performance Devices (Cornell, NY, 2000)*